

Transformations in the Iron–Manganese–Oxygen–Carbon System Resulted from Treatment of Solar Energy with High Concentration

Javier Mochón, Íñigo Ruiz-Bustanza, Alfonso Vázquez, Daniel Fernández, Julia María Ayala, María Florentina Barbés, and Luis Felipe Verdeja*

With the aim of achieving a “zero waste” generation in industry, particularly in that of iron and steel, we propose studying the option to compete in this type of process, making use of an energy that, in addition to being free of contaminants, is also inexhaustible as is the case of solar energy. Solar energy is currently polarized has its greatest use in the production of electricity, either via thermal solar or photovoltaic, and it is also used as a low temperature heat source for water heating applications in households, hospitals, or hotels. Solar energy, when properly focused, can offer great potential for application in basic operations as well as processes of a chemical or chemical–metallurgical nature used for the obtaining, manipulation, and finishing of metals. Moreover, much waste from the iron and steel industry, make up a by-product whose exploitation requires high energy consumption in order that, either attempts are made to recycle them directly, or they are attempted to be taken advantage by feeding them, together with the conventional load, in reduction ovens. High temperature concentrated thermal solar energy could permit, on one hand, the generation of a high quality product (free of impurities which are detrimental to the process) using clean energy, and, thusly, fulfill the goal of achieving a “zero waste” generation.

1. Introduction

Nowadays, there is a growing commitment to increase efforts towards worldwide development which are conditioned by environmental protection and sustainable development policies. In this context, we propose a search for new energy alternatives to be used in a variety of primary production processes which are less aggressive towards nature. In the case of the iron and steel industry, this possibility arises for via the use of high temperature concentrated solar thermal energy within a production

process which is characterized by the generalized existence of endothermic reactions.

Concentrated solar energy for the treatment and recycling of materials from the iron and steel industry can be used both directly and indirectly:

- For indirect use of solar energy: In this case we need the help of a fluid that contacts and exchanges heat with the load that is to be processed. This possibility was studied by Ruiz-Bustanza et al.^[1] and showed the feasibility of reducing hematite (Fe_2O_3) to magnetite (Fe_3O_4) in a fluid bed solar oven via the use of mill scale (a steel industry by-product) as a raw material.
- In direct use on raw material: In this case, a high energy circular radiating lamp, with a radius of several millimeters, impacts on the charge to be treated in order to reach the reaction temperature. In this article, we discuss the results obtained from the use of this technology on the carbothermic reduction of iron oxides^[2,3] and manganese oxides.^[4–6]

The tests and results presented here are part of an overall project that aims to study the possibility of using solar concentrated thermal energy in the processing and recycling of raw materials-waste generated by the chemical, metallurgy, and iron and steel industries. Waste

[*] J. Mochón, Í. Ruiz-Bustanza

Department of Primary Metallurgy, National Center for Metallurgical Research CENIM – CSIC, Avda. Gregorio del Amo, 8, Madrid 28040, Spain

A. Vázquez

Department of Surface Engineering, Corrosion and Durability, National Center for Metallurgical Research CENIM – CSIC, Avda. Gregorio del Amo, 8, Madrid 28040, Spain

D. Fernández, J. M. Ayala, M. F. Barbés, L. F. Verdeja

Group of Investigation in the Iron and Steel Industries, Metallurgy and Materials, School of Mines, University of Oviedo, C/Independencia 13, 33004 Oviedo, Asturias, (Spain) Associated Unit to CENIM-CSIC, Spain

Email: lfv@uniovi.es

www.uniovi.es/sid-met-mat.

DOI: 10.1002/srin.201300377

generated in blast furnaces, in steelworks (BOF or electrical)^[7] or in electric furnaces used for the production of ferromanganese are, in principle, considered suitable candidates.^[8]

Potentially, waste from the iron and steel industry can be used as complementary raw materials – good auxiliaries for obtaining pig iron,^[7] DRI (direct reduced iron),^[7] or for the production of ferroalloys.^[8] One of the problems posed by massive recycling of the above mentioned waste is that sintered products – the agglomerates that are attempted to be made – do not reach the physical, chemical, and mechanical specifications required for raw materials that are commonly used in the modern steel industry. Therefore, in some cases, it is not even possible to achieve 1.00% of waste in the load. The high-concentration solar competition could become a very useful technology for the transformation of these wastes, difficult to recycle using conventional processes, into sintered raw materials having a compatible quality to those required by current demands and production standards.^[9]

2. Experimental Method

Prior to treating the complex wastes from the iron and steel industry, we decided to carry out an experimental evaluation of the behavior of the prepared samples with high purity chemical reagents for processing with solar thermal energy directly applied to the sample.

2.1. Description of the Facilities

The reduction trials were carried out at the Vertical Axis Solar Energy concentration facilities located in Odeillo, France, belonging to Centre National de la Recherche Scientifique (CNRS).

The basis of this vertical shaft solar concentrator is explained in the diagram of **Figure 1a**. The solar oven at Odeillo is based on solar rays striking a heliostat, which follows the path of the sun and reflects the rays at a 2.0 m diameter concentrator parabola which makes solar radiation converge at a focal point with a dimension of approximately 12.2 mm in diameter (The spot is slightly wider than the width of the crucible to affect the entire load perfectly, in case of small deviations of the spot) (Figure 1b). The power density of the incident radiation, which is of the order of 800–1000 W m⁻², thus increases by four orders of magnitude to values of 1040–1650 W cm⁻².^[6,10,11]

The system is located on a cantilever in order for the solar radiation to be reflected by the heliostat and enter through the balcony floor (Figure 1a). There is a horizontal venetian blind on this floor whose slats that can rotate on a horizontal plane thus positioning them in either a parallel or normal manner. In this way it is possible to control

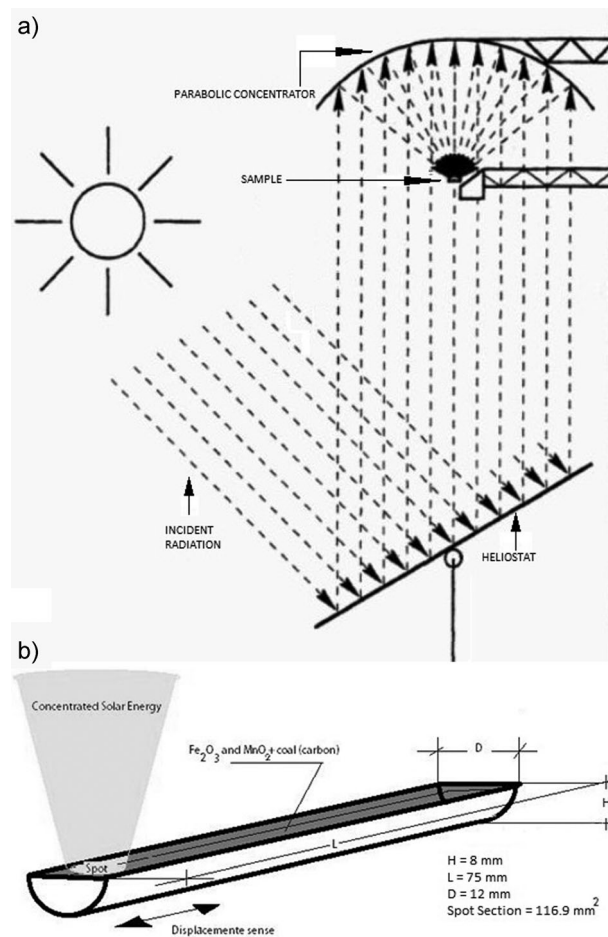
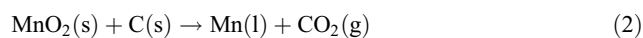
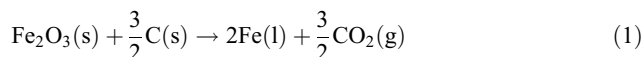


Figure 1. a) Basic diagram of the vertical shaft solar concentrator. b) Diagram of carbothermic reduction process of iron and manganese oxides with solar energy of high concentration in refractory crucible.

incident radiation, thus increasing or decreasing the power density that is finally concentrated on the sample.

2.2. Sample Preparation

Various mixtures of Fe₂O₃ and carbon are prepared in order to study the possibility of obtaining iron via direct reduction; Fe₂O₃, MnO₂, and carbon mixtures were also prepared, in order to obtain ferromanganese; the amount of carbon necessary to carry out each of the two reductions has been calculated by taking into account of the following stoichiometric relations:



The samples that were tested in the solar oven contain various excesses of reduction agents, varying in percent by

weight: 10%, 15%, 25%, or 40% over the stoichiometric amount by weight required for reactions (1) and (2) (Table 1).

The iron oxide powder used was 100% pure (Prolabo (Rectapur)) and had a particle size of $6.7\ \mu\text{m}$ (d_{50}). This was mixed with 100% pure carbon dust (Panreac) with a particle size of $10.2\ \mu\text{m}$ (d_{50}), with the indicated varying excesses with respect to the reduction stoichiometric value.

The mixtures, with masses around 0.80–2.50 g (Table 1), were placed in laboratory silicon-aluminous ceramic crucible with a length of 75 mm, a width of 12 mm, and a depth of 8.0 mm (Figure 1b and 2a), which were manually cold compacted using a spatula to optimize the contact between reactants and to try to minimize the potential risk of material projections throughout the trial.

Thermocouples were placed at the bottom of the reaction mass through some perforations in the bottom of the crucibles in order to find the temperatures reached by modifying the conditions of each test (Figure 2b; T2, T3, and T4 thermocouples positions were outside of the crucible (indirect measure of temperature), and T1 thermocouple position was into the sample (direct measure of the temperature)). The test crucible is placed on an alumina plate (Figure 2a) on an XYZ table which is moved longitudinally in the plane XY in order to pass the length of the crucible via the focal point to receive the power density available in each case.

2.3. Operating Procedure

The variables used in the tests were:

- Power density of the radiation applied to the sample. The power density was controlled, in relation to the existing levels, opening the louvers to a greater, or lesser degree which were located between the heliostat and the parabolic concentrator and/or defocusing the sample position on the Z axis.
- Sample displacement speed under the focal point. This speed remained variable throughout the route, especially in the beginning, to allow time for initial preheating of

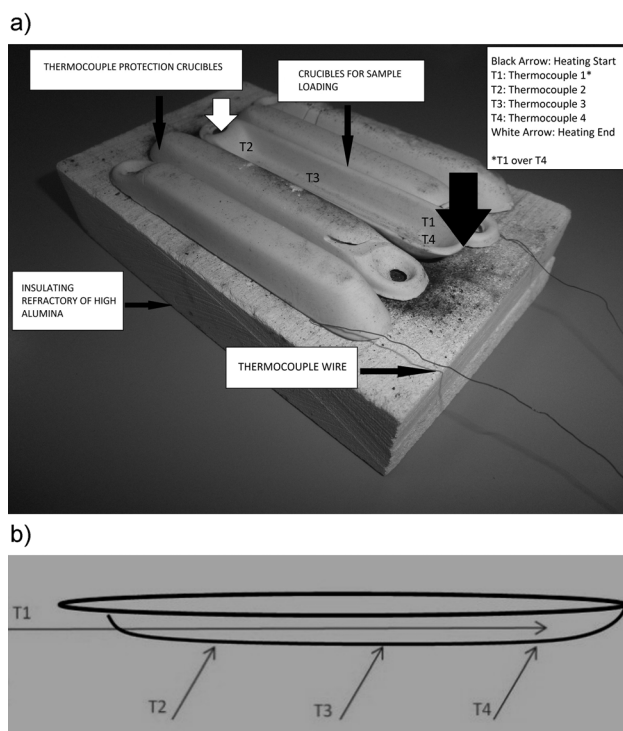


Figure 2. a) Experimental device for the test, and positions of thermocouples in the crucible. b) Positions of the thermocouples in the sample.

the end. The sample displacement speed is related to the heat flow, and with the temperature of the sample.

- Relationship between the amount of oxide and carbon reducer used.
- Different amount of reactive mass.

3. Experimental Results and Discussion

The external experimental conditions under which the trials were conducted, with greater or lesser levels of

Sample	Reagents chemical composition	Displacement speed [mm s^{-1}]	Power [kW m^{-2}]	Maximum temperature (thermocouple) [$^{\circ}\text{C}$]
Trial 10 Test 1	Fe_2O_3 (1.23 g) + 125% C (0.17 g)	0.76	9860	Undetermined
Trial 12 Test 4	Fe_2O_3 (1.62 g) + 125% C (0.23 g)	0.35	6950	Undetermined
Trial 20 Test 4	Fe_2O_3 (1.75 g) + 125% C (0.25 g)	0.30	9680	1339
Trial 25 Test 1	Fe_2O_3 (0.94 g) + 140% C (0.16 g)	0.25	10 100	1328.2
Trial 36 Test 2	Fe_2O_3 (0.62 g) + MnO_2 (1.35 g) + 110% C (0.23 g)	0.25	9600	1160
Trial 39 Test 3	Fe_2O_3 (0.55 g) + MnO_2 (1.2 g) + 125% C (0.25 g)	0.25	8590	1180.9

Table 1. Reagents of the samples and the samples analyzed variables.

insolation, varied greatly. There were days when sunshine was only at 650 W m^{-2} and others when it reached 1030 W m^{-2} . The ability to act upon those controls that were available at the facilities, essentially aperture, scanning speed, and blur on the Z axis, allowed for testing with applied power density and applied total energy per unit of mass, which was very different from one case to another. The maximum temperature reached in the thermocouples was $1400 \text{ }^\circ\text{C}$ (Figure 3), and the sample was heated during 250 s as we can see in Figure 3. The sample was heated in a short time, because the kinetic constant of the process is of Arrhenius type (exponentially activated with temperature), thus, with the high temperatures reached, the reaction times are short. The reaction time can be controlled with the sample displacement speed (the length of the sample is a constant value, so if we change the sample displacement speed, we will change the action time of the focus over the sample).

It should be noted that in tests carried out in parallel to the tests described, work took place on the development of a computer program in MATLAB base supported by the finite element method that provided guidance on the range of times and temperatures for the high energy direct solar radiation tests (Figure 1b).^[12,13]

It would thus be possible to have a more precise idea about the variables controlling experiments at Odeillo, and moreover, to correct the model created to adopt it to the experimental measurements of the thermocouple temperatures with a higher level of accuracy (Figure 2a and b).

While performing tests, it was possible to follow the progress of the reaction using special crystals like the type used in welding to protect one's eyes. It was observable that, depending on the experimental conditions, this reduction reaction did not occur when the reaction took place in a relatively calm or more tumultuous manner, either due to the sparks from glowing carbon particles leaping from the reaction mass, or when the temperature was insufficient.

Once the test had finished and the sample had cooled, it was observable to the naked eye whether or not there had

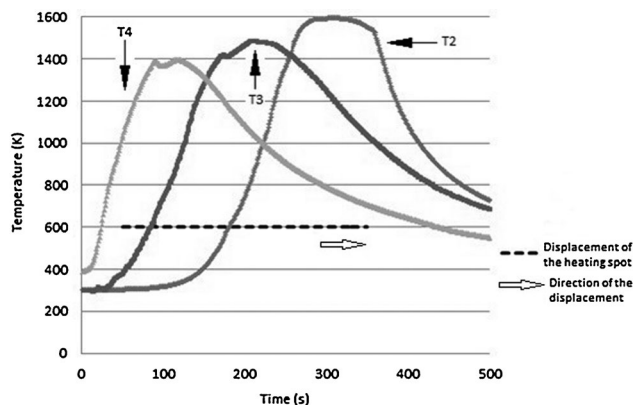


Figure 3. Temperature profile of the essay Trial 25 Test 1.

been a reduction of the iron oxide due to the existence of a mass of molten iron, either continuous or as pellets of varying sizes^[9]. Table 1 and 2 shows the performance data for iron obtained with respect to the stoichiometry for various test conditions (speed and applied power density), and for the various cases of greater or lesser reducer excess on the stoichiometric.

An analysis of the products obtained by X-ray diffraction was carried out, using the X Powder software and the PDF2 database. Table 1 lists the samples that were finally selected for analysis from the total of tests performed: Four samples of Fe_2O_3 and carbon, two samples of Fe_2O_3 , MnO_2 and carbon. In addition, the table shows, a part from the reducer excesses, the conditions chosen for the various variables: metal oxide ratio to reduced, the load displacement speed and the incident beam power.

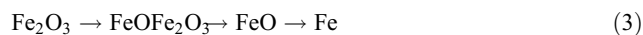
The results from the characterization study allow us to classify the products obtained into five categories (the \pm in the tables indicate the confidence interval of the amount of each product):

3.1. Metallic Products

Table 2 shows the results achieved as to the degree of metallization of the products. We observe that, of the six samples analyzed, metallic iron from the direct reduction of iron ore can be found in three of them.^[2,14] In any event, the quantities obtained are very small, indicating that complete reduction is not verified in any of the cases analyzed. For the situations in which an Fe_2O_3 and MnO_2 mix is employed, the results of X-ray diffraction did not ensure the presence of ferromanganese in the final product. We therefore conclude that the desired results are only partially achieved, since the presence of direct reduction iron is ensured only in some samples. Comparing the data of Table 1 and 2, we conclude that the best metallizations are achieved in cases in which the radiation power is maximum and the rate advance of the crucible is low (0.25 mm s^{-1}). The recorded temperatures, via, thermocouples are highest under these conditions.

3.2. Oxidized Materials

The reduction sequence for oxides, both for iron and manganese is:



The results in Table 3 and 4 confirm the presence of the various oxides previously shown in the final sample. The presence of a greater or lesser degree of metallization in the final product will depend on the amount of FeO,

Sample	Fe	FeMn ₃ (Solid Solution)	FeMn ₄ (Solid Solution)
Trial 10 Test 1	1.1 ± 1.1%	–	–
Trial 12 Test 4	1.30 ± 1.2%	–	–
Trial 20 Test 4	3.80 ± 1.9%	–	–
Trial 25 Test 1	6.00 ± 3.8%	–	–
Trial 36 Test 2	1.20 ± 1.2%	2.80 ± 2.8%	1.10 ± 1.1%
Trial 39 Test 3	2.70 ± 2.7%	3.60 ± 3.6%	3.00 ± 3.0%

Table 2. Metallic iron, FeMn₃ (Solid Solution), and FeMn₄ (Solid Solution) quantities.

MnO, and C that is reached in the final stage of the reduction process. If any of these three reagents did not exist, the final metallization sample would be nil.

Finally, it is interesting to mention Trial 20 Test 4 here. This deals with the trial where the higher powers are managed and higher temperatures are reached (Table 1), the diffraction analysis shows that it is the one that yields the highest amount of metallic iron even though it also presents the greatest amount un-reacted hematite (Fe₂O₃) (Table 4). This could indicate that only the hematite that was able to be reduced to FeO (stoichiometric) and FeO_x (wustite) (Table 3), is subsequently *the one* that would be able to reach a metallic state (Table 2).

3.3. Elemental Carbon

In all the samples that were analyzed, the final carbon quantities used as reducer are virtually zero, thus indicating that the amount of this was deficient for the process that was aimed to be accomplished.

The fact that the tests are carried out outdoors will favor carbon combustion with oxygen. In case of a controlled atmosphere (reductant), the levels of metallization achieved would be higher.^[6,10,11] It was decided to use a simplified experimental device to dismiss with the use, for example, of a transparent hood to the solar radiation to prevent the sample from direct contact with air and,

Sample	FeO	FeO _x (wustite)	Fe ₃ O ₄	MnO
Trial 10 Test 1	38.7 ± 0.5%	35.2 ± 0.6%	11.4 ± 1.3%	–
Trial 12 Test 4	25.80 ± 1.0%	35.70 ± 1.0%	24.80 ± 0.3%	–
Trial 20 Test 4	19.60 ± 1.5%	22.10 ± 1.5%	12.30 ± 0.6%	–
Trial 25 Test 1	7.70 ± 3.6%	–	7.60 ± 3.6%	–
Trial 36 Test 2	6.10 ± 2.7%	–	2.60 ± 2.2%	23.00 ± 0.9%
Trial 39 Test 3	3.00 ± 3.0%	–	21.00 ± 2.3%	9.40 ± 5.6%

Table 3. Partially reduced quantities of products.

Sample	Fe ₂ O ₃	MnO ₂	Carbon
Trial 10 Test 1	9.4 ± 1.3%	–	0.6 ± 0.6%
Trial 12 Test 4	4.50 ± 1.1%	–	0.20 ± 0.2%
Trial 20 Test 4	30.10 ± 1.3%	–	1.10 ± 1.1%
Trial 25 Test 1	24.6 ± 2.8%	–	5.90 ± 3.5%
Trial 36 Test 2	0.60 ± 0.6%	–	1.00 ± 1.0%
Trial 39 Test 3	3.10 ± 3.1%	1.90 ± 1.9%	3.10 ± 3.1%

Table 4. Quantities of the starting reactants into products.

instead, it would maintain a conditioned atmosphere with reducer and inert gases thus favoring the degree of metallization of the products.^[11] The non-use of the hood is because it is necessary to identify the trial with an industrial sintering process where the atmosphere is not controlled, unlike the tests performed on an indirect use analysis, in which mill scale is used, where an atmospheric control is performed.^[1] That is, it looks for operating conditions similar to those in the industrial sintering process.^[9]

3.4. Metallic Carbides

The formation of cementite, Fe₃C, is thermodynamically favorable ($\Delta_r G^\circ < 0$),^[14–16] as it would be possible see if it is introduced in the next equation the work's temperature:

$$\Delta_r G^\circ(T) = 125.47 - 0.1386 T (\text{kJ/mol C})$$

It would not, therefore, be surprising to find the presence of varying amounts of the carbide in the samples. **Table 5** shows the percentages of such products in the samples; the presence of iron carbide (Fe₃C, Fe₂C, and FeC) is significantly higher than the degree of metallization of iron and ferromanganese found. We can, therefore, certify that the experimental conditions at Odeillo favor the presence of these products.

The presence of a greater amount of iron carbides in the final products is logical due to the high temperatures, (Table 1), and to the fact that the concentration of the reactants for the formation of carbides is higher, if compared with that of those reactions that evolve towards the formation of metallic iron and manganese.

For the formation of metal products, the necessary reagents are the most reduced oxides (FeO and MnO) and the carbon monoxide (CO), whereas for the synthesis of carbides, only the presence of carbon monoxide in the gas is necessary. So, in the test conditions, it is possible to obtain metallic carbides directly from the initial iron oxide (Fe₂O₃) in presence of carbon monoxide.

3.5. Other Products

Apart from the compounds mentioned so far, X-ray diffraction spectrum would indicate to us the presence of other compounds:

- i. Double oxides of manganese and iron: We can see this for the sample corresponding to Trial 36 Test 2, where the following compounds appear:

Jacobsite (MnFe₂O₄) : 26.60 ± 1.0%

Iwakiite (MnFe₂O₄) : 27.10 ± 1.0%

These oxides would make up part of the previous reduction phases for the formation of the ferromanganese which is the object of the trial.

- ii. Silicates: In Trial 39 Test 3 the presence of the compounds below are observed as a result of diffraction spectrum analysis:

Tephroite (Mn₂SiO₄) : 17.20 ± 3.2%

Fayalite ((FeMn)₂SiO₄) : 7.30 ± 6.1%

These silicates appeared due to the interface between the melt and the silicon-aluminous refractory and a reaction occurred between them. Additionally, it is significant to find that in some of the trials these crucibles appear deformed (**Figure 4**), indicating that higher temperatures than the eutectic of the silicon-aluminous refractory^[17–19] have been reached.

The thermocouples (**Figure 2b**) that were introduced into the samples gave readings between 1000 and 1400 °C (**Figure 3**) (firstly, we thought that it was better the direct measure of the temperature (T1 in the **Figure 2b**) than the indirect measures (T2, T3, and T4 in the **Figure 2b**), but the essays show us that the stability of the sample and the temperature measure results were better in the indirect measures). The incidents that we have just stated allow us to assume that the

Sample	Fe ₃ C	Fe ₂ C	FeC
Trial 10 Test 1	2.7 ± 1.6%	0.5 ± 0.5%	–
Trial 12 Test 4	1.10 ± 1.1%	4.50 ± 1.2%	1.10 ± 1.1%
Trial 20 Test 4	0.90 ± 0.9%	0.80 ± 0.8%	0.70 ± 0.7%
Trial 25 Test 1	4.40 ± 3.9%	10.10 ± 3.4%	6.10 ± 3.7%
Trial 36 Test 2	4.20 ± 2.9%	2.80 ± 2.8%	0.50 ± 0.5%
Trial 39 Test 3	8.50 ± 6.0%	3.80 ± 3.8%	2.00 ± 2.0%

Table 5. Iron carbides in the sample.

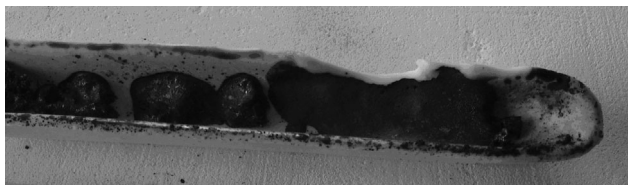


Figure 4. Final result for the Trial 39 test 3.

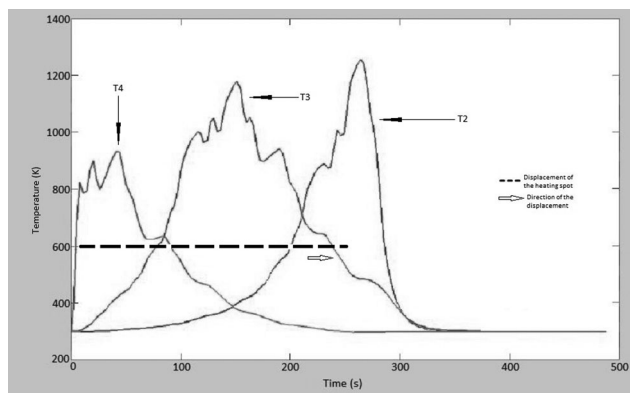


Figure 5. Temperature profile of the Trial 25 Test 1 (simulation).

temperatures reached during the trials at the top area of the load of the crucibles were higher than those recorded by the thermocouples. Correlating the information reflected by the thermocouples with the results that the simulation provided us, we can say that the temperatures were similar to those known for the simulation stage (Figure 5).

4. Conclusions

Starting from chemically pure oxidic raw materials, by way of directly applying a solar energy beam with heat flows between 1040 and 1650 W cm^{-2} to the samples, and using carbon as a reducer ($>99\%$ C), we have obtained the following conclusions:

By direct application of the high temperature concentrated solar thermal, it is possible to obtain reduced products from loads consisting only of iron oxide (III), and others composed of an iron oxide mix (III) and manganese oxide (IV). Nevertheless, the obtaining of metal products (small metallic nodules) reaches low performance. While the reduction process is favored by the high temperatures, it competes with other alternatives (carbon oxidation, for example) that prevent it from achieving a high level of performance.

The gasification–combustion kinetics of carbon plays an important role in the results obtained. The

use of any reduction atmosphere would allow for the improvement of metallization in the final product. Similarly, it is possible to consider working with higher percentages of carbon, although it has been tested under specific experimental conditions tested in the furnace at Odeillo, that the experimental results do not vary significantly.

From the results obtained in the tests carried out, we can lay the foundations for the implementation of new processes that may have as a raw material with those waste products resulting from the various iron and steel operations and processes. It is feasible to consider carrying out experiments on the interaction between high heat flow direct solar energy in blast furnace dusts, or on waste from the production of ferromanganese (electric oven reduction dust resulting from the production of ferromanganese (80% Mn, 7% C)). The interaction between solar energy and waste products from the iron and steel industry can promote agglomeration–consolidation (sintering) of waste, as well as the removal of annoying volatile contaminants.

Acknowledgements

The authors wish to thank the Processes, Materials, and Solar Energy Laboratory (PROMISE-CNRS), the French research centre under the Centre National de la Recherche Scientifique (CNRS), and CENIM-CSIC for their cooperation in conducting the investigation.

Received: October 2, 2013;

Published online: March 24, 2014

Keywords: Concentrated solar thermal energy; Oxide reduction; Iron products; Ferromanganese

References

- [1] I. Ruiz-Bustinza, I. Cañadas, J. Rodríguez, J. Mochón, L. F. Verdeja, F. García-Carcedo, A. J. Vázquez, *Steel Res. Int.* **2013**, *84*(3), 207.
- [2] A. Steinfeld, Y. E. A. Fletcher, *Energy* **1991**, *16*(7), 1011.
- [3] J. P. Murria, A. Steinfeld, E. A. Fletcher, *Energy* **1995**, *20*(7), 695.
- [4] M. Kumar, S. Ranganathan, S. N. Sinha, *INFACON XI (Innovations in Ferro Alloy Industry)*, The Indian Ferro Alloy Producers Association, **2007**, p. 241.
- [5] N. J. Welham, *Int. J. Miner. Process.* **2002**, *67*, 187.
- [6] R. Kononov, O. Ostrovski, S. Ganguly, *ISIJ* **2009**, *49*(8), 1107.
- [7] A. Babich, D. Senk, H. W. Gudenau, T. Th. Mavrommatis, *Ironmaking*, Department of Ferrous Metallurgy, RWTH Aachen University, Aachen, **2008**, p. 50.

- [8] S. E. Olsen, M. Tangstad, T. Lindstad, *Production of Manganese Ferroalloys*, Tapir Akademisk Press, Trondheim **2007**, p. 19–69
- [9] A. Cores, L. F. Verdeja, S. Ferreira, I. Ruiz-Bustinza, J. Monchón, *Dyna* **2013**, *180*, 152–171.
- [10] T. Osinga, U. Frommherz, A. Steinfeld, C. Wieckert, *J. Sol. Energ. Eng.* **2004**, *126*, 633.
- [11] C. Sánchez Bautista, A. Ferriere, G. P. Rodríguez, M. López-Almodovar, A. Barba, C. Sierra, A. J. Vázquez. *Intermetallics* **2006**, *14*, 1270.
- [12] A. A. Fernández, L. F. Verdeja, *Práctica y problemas de siderurgia*, Fundación Luis Fernández Velasco, Oviedo, **2000**.
- [13] C. Sánchez Bautista, G. P. Rodríguez, A. Ferriere, *Surf. Coat. Technol.* **2008**, *202*, 1594.
- [14] J. Sancho, L. F. Verdeja, A. Ballester, *Metalurgia Extractiva. Volumen II. Procesos de obtención*, Síntesis, Madrid **2000**, p. 22.
- [15] Y. A. Çengel, M. A. Bodes, *Termodinámica*, McGraw-Hill, México D. F. **2004**, p. 794.
- [16] A. Ballester, L. F. Verdeja, J. Sancho, *Metalurgia Extractiva. Volumen I. Fundamentos*, Síntesis, Madrid, **2000**, p. 116.
- [17] A. L. Cavalieri, P. Pena, S. de Aza, *Bol. Soc. Esp. Ceram. Vidr.* **1990**, *29(3)*, 171–176.
- [18] L. F. Verdeja, J. P. Sancho, A. Ballester, *Materiales refractarios y cerámicos*, Síntesis, Madrid **2008**.
- [19] J. A. Pero-Sanz Elorz, *Ciencia e ingeniería de materiales. Estructura, transformaciones, propiedades y selección*. CIE Dossat-2000, Madrid, p. 380.